Synthesis and pharmacokinetic study of a ^{11}C-labeled cholesterol 24-hydroxylase inhibitor using 'in-loop' [^{11}C]CO_2 fixation method

Zhen Chen[a] , Jiahui Chen[a] , Natalia Mast[b] , Jian Rong[a] , Xiaoyun Deng[a] , Tuo Shao[a] , Hualong Fu[a] , Qingzhen Yu[a] , Jiyun Sun[a] , Yihan Shao,[c] Lee Josephson[a] , Thomas Lee Collier[a] , Irina Pikuleva[b] , and Steven H. Liang[a,] ∗

[a]*Division of Nuclear Medicine and Molecular Imaging, Massachusetts General Hospital & Department of Radiology, Harvard Medical School, Boston, MA, 02114, USA.*
[b]*Department of Ophthalmology and Visual Sciences, Case Western Reserve University, Cleveland, OH, 44106, USA*
[c]*Department of Chemistry and Biochemistry, University of Oklahoma, Norman, Oklahoma 73019, United States*

ARTICLE INFO

keywords:
cholesterol 24-hydroxylase
CYP46A1
Alzheimer's disease
positron emission tomography
[^{11}C]CO_2 fixation

ABSTRACT

Cholesterol 24-hydroxylase is a monooxygenase encoded by CYP46A1, which is specifically expressed in the brain where it controls cholesterol elimination by producing 24*S*-hydroxylcholesterol (24-HC) as the major metabolite. Selective blockade of CYP46A1 activity may suppress neuronal cell death, Aβ deposition and p-tau accumulation by decreasing 24-HC formation, which thereafter serves as potential therapeutic pathway for Alzheimer's disease. In this work, we showcase the efficient synthesis and preliminary pharmacokinetic evaluation of a novel cholesterol 24-hydroxylase inhibitor **1** by positron emission tomography study.

1. Introduction

Alzheimer's disease (AD) is a long-term neurodegenerative disorder that ranks sixth in the leading cause of all deaths in the United States and features amyloid β protein (Aβ) deposition and neurofibrillary tangles composed of aggregated phosphorylated tau protein (p-tau).[1] To date, an estimated 6% of 65-year or older people in the world are suffering from AD, which approximately accounts for 95% of AD cases. Despite tremendous research efforts towards AD, the underlying cause of AD remains elusive, and no treatment has been disclosed to stop or reverse the AD progress.

Recent studies have demonstrated that abnormalities of cholesterol homeostasis in the brain are strongly associated with several neurodegenerative diseases, such as AD, Parkinson's disease (PD) and Huntington's disease (HD).[2-6] As an important structural component of myelin as well as membranes of neurons and glial cells, cholesterol plays a central role in the process of dendrite outgrowth and myelination, maintenance of stability of microtubules, and synaptogenesis.[7] In the brain, cholesterol is mainly metabolized into 24*S*-hydroxylcholesterol (24-HC) by cholesterol 24-hydroxylase (CH24H) for elimination. CH24H is a monooxygenase, which is encoded by cytochrome P450 enzyme CYP46A1. It was reported that CYP46A1 polymorphism in the brain, which is deeply linked with increased Aβ and p-tau expression, could be a risk factor in AD pathology.[8, 9,10] In addition, 24-HC could lead to cell death and short-term memory impairment.[11-13] Therefore, modulation of CYP46A1 activity may suppress neuronal cell death, Aβ deposition and p-tau accumulation by decreasing 24-HC formation, which thereafter serves as potential therapeutic pathway for AD. Mast et al have demonstrated that a series of marketed drugs could be re-purposed as potent CYP46A1 modulators including tranylcypromine, thioperamide, voriconazole, clotrimazole, and fluvoxamine.[14-17] Some of these compounds were co-crystallized with CYP46A1 to elucidate their molecular interactions.

Positron emission tomography (PET) is a sensitive, quantitative, and non-invasive nuclear imaging tool to provide diagnostic information about the biological processes under disease conditions.[18-20] PET studies of CYP46A1 would allow to better understand in vivo biochemistry and physiology of cholesterol homeostasis, help to accelerate the translation of CYP46A1 modulators in clinical trials, as well as offer an in-depth insight into AD. Recently, we developed a facile "in loop" [^{11}C]CO_2

∗ Corresponding author. e-mail: Liang.Steven@mgh.harvard.edu

fixation technology, which directly takes advantage of an automated apparatus to enable ^{11}C-carbonylation in high efficiency.[21-24] With this technology, we and other groups have successfully synthesized a series of PET tracers, such as [^{11}C]SL25.1188, [^{11}C]JNJ1661010 and [^{11}C]MAGL-2-11.[23, 25-27] As our combined interest in the CYP46A1-targeted PET ligand development and application of 'in-loop' [^{11}C]CO_2 fixation, we present herein the facile synthesis of ^{11}C-labeled compound **1**, which was recently patented as a potent CYP46A1 inhibitor (**Figure 1**).[28, 29] Pharmacological and physicochemical evaluation of compound **1**, as well as pharmacokinetic profiling via in vivo PET imaging and whole-body biodistribution experiments of [^{11}C]**1** are reported in this work.

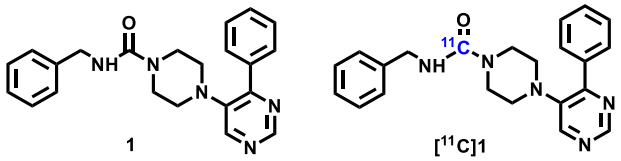

Figure 1. Chemical structure of CYP46A1 inhibitor **1** and [^{11}C]**1**

2. Result and discussion

2.1 Chemistry

The synthetic route of CYP46A1 inhibitor **1** is shown in **Scheme 1**. In brief, we used commercially available tert-butyl 4-(4-phenylpyrimidin-5-yl)piperazine-1-carboxylate **2** as the starting material. Trifluoroacetic acid (TFA)-promoted removal of the *tert*-butyloxycarbonyl (Boc) group proceeded smoothly to give free amine **3** in 99% yield, which also served as the labeling precursor for follow-up [^{11}C]CO_2 fixation. Subsequent installation of benzylaminocarbonyl group into **3** was readily achieved with the combination of benzylamine, triphosgene and *N*,*N*-diisopropylethylamine (DIPEA) in THF. In all, the desired CYP46A1 inhibitor **1** was synthesized in 52% yield.

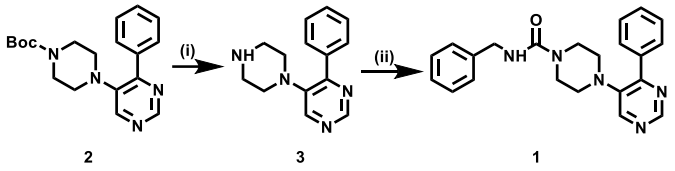

Scheme 1. Synthesis of CYP46A1 inhibitor **1**. (i) TFA, CH_2Cl_2, rt, 8 h, 99% yield; (ii) benzylamine, triphosgene, DIPEA, THF, rt, 30 min, 52% yield. TFA = trifluoroacetic acid, DIPEA = *N*,*N*-diisopropylethylamine, THF = tetrahydrofuran.

2.2 Pharmacology and physiochemical property

We select compound **1** from a patent literature describing therapeutic drug molecules towards CYP46A1 for the treatment of neurodegenerative diseases.[28, 29] The compound showed 95% inhibitory activity towards CYP46A1 at 1 μM concentration and possessed a carbamide (urea) moiety which is amenable for radiolabeling using our 'in-loop' [^{11}C]CO_2 fixation.[21-24] Subsequent in silico calculation also indicated a favorable value of 60.3 Å for topological polar surface area (tPSA). Multi-parameter optimization (MPO) has been widely utilized in the CNS drug discovery to evaluate brain permeability.[30] Our test compound 1 showed a MPO score of 4.9, which together with other prediction indicated that **1** may have high likelihood to penetrate the blood-brain barrier. Experimentally, compound **1** was subjected to potency evaluation towards CYP46A1 in vitro with our previously developed method.[16, 31] Briefly, purified CYP46A1 (d(2-50)CYP46A1-4His) was reconstituted with varying concentrations of compound **1** , rat NADPH cytochrome P450 oxidoreductase and cholesterol. The hydroxylation reaction was started by nicotinamide adenine dinucleotide phosphate (NADPH) at 37 °C, and maintained at the same temperature for 30 minutes. Enzymatic reaction was terminated by addition of dichloromethane. The hydroxylation products extracted with dichloromethane were then subjected to GC-MS (gas chromatography-mass spectrometry) analysis with 24-OTMS d_7-cholesterol as internal standard. As depicted in **Figure 2**, the Ki of compound **1** was determined to be 7.3 ± 0.1 μM. We postulated the discrepancy of binding affinity of compound **1** could be derived from different measurement methods. In all, although it is certain that a more potent compound is necessary to demonstrate high binding potential in PET study, a radiochemical application of our [^{11}C]CO_2 fixation method based on compound [^{11}C]**1** were carried out to provide preliminary pharmacokinetic profiling as an entry point for further design CYP46A1 ligands.

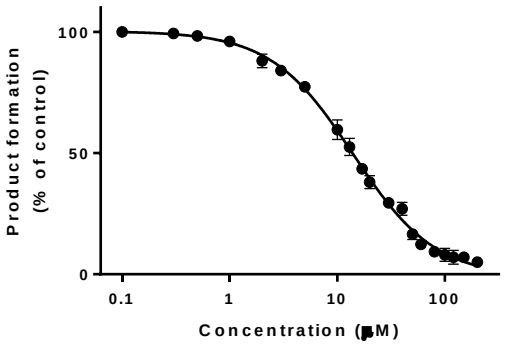

Figure 2. The concentration-response curve of **1** for inhibition of cholesterol 24-hydroxylation by CYP46A1.

2.3 Radiosynthesis and lipophilicity measurement

In virtue of the urea group, radiosynthesis of compound **1** could be directly carried out via our previously developed 'in-loop' [^{11}C]CO_2 fixation strategy.[23, 24, 26] As shown in **Figure 3**, [^{11}C]CO_2 was first reacted with benzylamine to form a carbomate intermediate [^{11}C]**5** with BEMP as the [^{11}C]CO_2 trapping reagent. $POCl_3$-mediated dehydration of [^{11}C]**5** provided the isocyanide species [^{11}C]**6**, which, upon quenched with secondary amine **3**, yielded the desired radioligand [^{11}C]**1**. It was found that the efficiency of this reaction is closely associated with the amount of benzylamine. Using 4.6 μmol of benzylamine, the desired product [^{11}C]**1** was obtained in a poor radiochemical conversion (4% RCC), whereas the side symmetric product [^{11}C]**7** was formed in 80% RCC (entry 1, **Table 1**). Decreasing the amount of benzylamine to 0.92 μmol successfully suppressed the formation of side product [^{11}C]**7**, and the RCC of [^{11}C]**1** increased to 45% (entry 2). Further decrease of benzylamine loading by 50% led to an increased RCC to 61% (entry 3). For comparison, we also performed a vial-based [^{11}C]CO_2 reaction for the radiosynthesis of [^{11}C]**1**. Unfortunately, merely trace product was obtained (entry 4), which further highlighted the advantage of our 'in-loop' [^{11}C]CO_2 fixation method. Ultimately, [^{11}C]**1** was isolated in 21% decay-corrected radiochemical yield (RCY) with excellent radiochemical purity (>99%) and high molar activity (>37 GBq/μmol). Excellent in vitro formulation stability was observed for [^{11}C]**1**, as evidenced by no radiolysis 90 min post formulation in saline containing 5% ethanol (**Figure 4**). Lipophilicity of a specific drug is an important index to evaluate its permeability of the blood-brain barrier (BBB) with a favorable range from 1.0 to 3.5.[32-34] The lipophilicity of [^{11}C]**1** (log*D*) was measured as 3.05 ± 0.02 via the 'shake flask' method, which is the liquid-liquid partition between phosphate buffered saline (PBS) and *n*-octanol.[35]

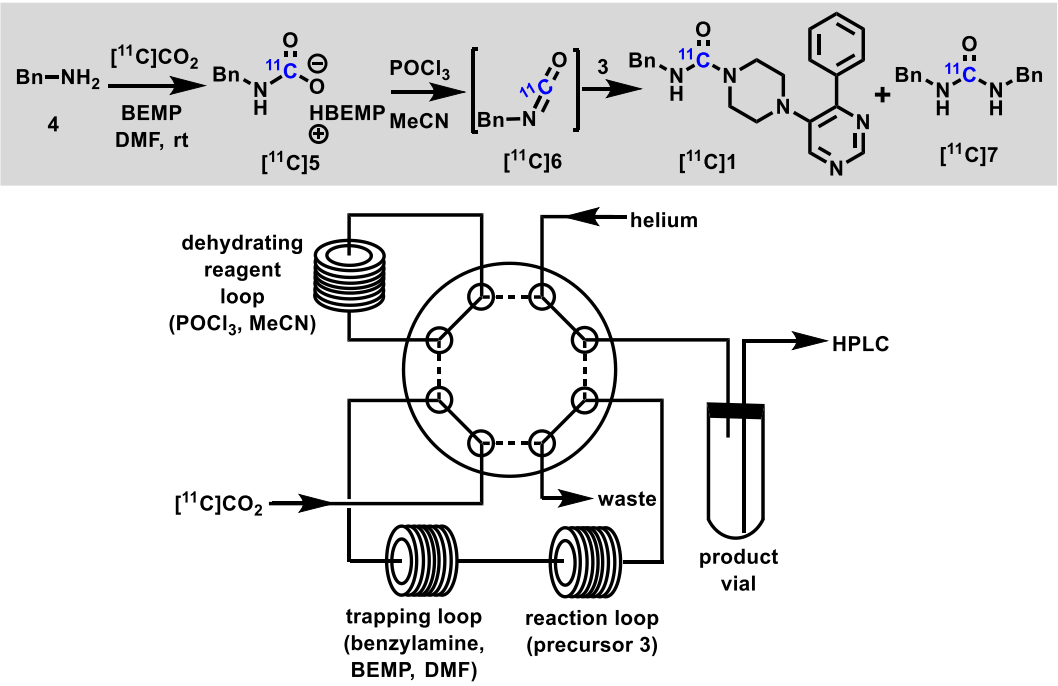

Figure 3. Schematic diagram of the "in loop" [^{11}C]CO_2-fixation module

Table 1. Optimization of reaction parameters for radiosynthesis of tracer [^{11}C]**1**.[a]

Entry	4 (μmol)	3 (μmol)	[^{11}C]CO_2 trapping (%)	RCC of [^{11}C]**1** (%)	RCC of [^{11}C]**7** (%)
1	4.6	8.4	>99	4	80
2	0.92	18.5	>99	45	35
3	0.46	18.5	>99	61 (21)[b]	12
4[c]	0.92	8.3	90	trace	trace

[a]Reaction conditions: loop A: benzylamine **4** and BEMP (2.5 μL, 8.6 μmol) in DMF (40 μL); loop B: **3** in DMF (50 μL); loop C: 0.2% $POCl_3$ (v/v, 1.1 μmol) in MeCN (100 μL) and additional 800 μL MeCN. [b]Decay-corrected radiochemical yield (RCY). [c]Reaction was conducted in a vial.

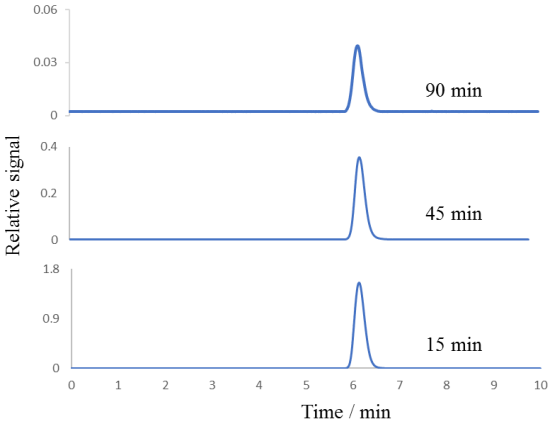

Figure 4. Stability of radioligand [^{11}C]**1** in saline containing 5% of ethanol.

2.4 PET imaging studies in mice

With [^{11}C]**1** in hand, we then performed dynamic PET acquisitions in CD-1 mice for 60 min. Representative PET images in the brain (0-60 min summed) and whole-body as well as time-activity curves (TACs) are shown in **Figure 5** and **Figure S1** in the Supporting Information. [^{11}C]**1** demonstrated limited brain uptake with a maximum standard uptake value (SUV) of 0.42 at 0.5 min, followed by a steady washout. Pretreatment of 2-phenylcyclopropan-1-amine (3 mg/kg), a known CYP46A1 inhibitor,[14] reduced the uptake of [^{11}C]**1** (~31% decrease of AUC, area under curve). These experiments indicated a marginal level of in vivo binding specificity for [^{11}C]**1**.

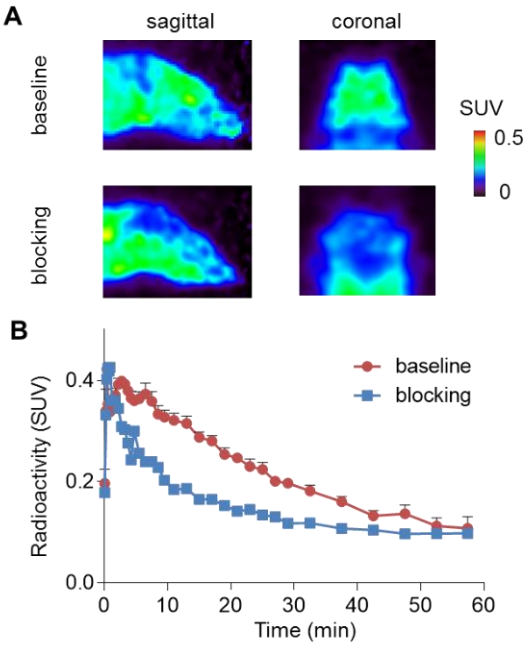

Figure 5. (A) Representative PET images of [^{11}C]**1** in mouse brain (0-60 min summed); (B) Time–activity curves of [^{11}C]**1** in mouse brain.

2.5 Whole-body ex vivo biodistribution studies

To further probe the uptake, biodistribution and elimination of [^{11}C]**1**, whole-body ex vivo biodistribution was carried out in mice at four time points (5, 15, 30 and 60 min) post intravenous (IV) injection of the radioligand. As shown in **Figure 5** and **Table S1** in the Supporting Information, tracer [^{11}C]**1** exhibited limited brain uptake, which is in line with the results from PET imaging studies. High radioactivity was accumulated in several organs including lungs, pancreas, small intestine, kidneys and liver (>10% ID/g, injected dose per gram of wet tissue), followed by fast washout. The radioactivity in small intestine reached a climax at 30 min followed by fast elimination, which together with high residue radioactivity in the small intestine and liver, suggested the urinary and hepatobiliary elimination pathway for [^{11}C]**1**.

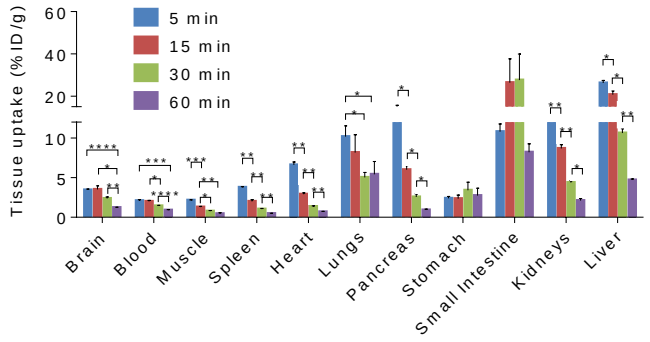

Figure 6. Whole-body ex vivo biodistribution studies of [^{11}C]**1** in mice at four different time points (5, 15, 30 and 60 min) post tracer injection. Data are expressed as % ID/g (mean ± SD; n = 4). Asterisks indicate statistical significance. $^{*}p < 0.05$, $^{**}p \leq 0.01$, $^{***}p \leq 0.001$, and $^{****}p \leq 0.0001$.

3. Conclusion

In this work, we have efficiently synthesized a novel CYP46A1 PET tracer [^{11}C]**1** in high radiochemical yield (21%), excellent molar activity (>37 GBq/μmol) and radiochemical purity (> 99%) using 'in-loop' [^{11}C]CO_2 fixation method. By PET imaging and ex vivo whole body distribution studies, we provided a pharmacokinetic profile (uptake, retention and clearance) of [^{11}C]**1** in major organs, of which the brain exhibited low uptake (0.4 SUV) and marginal binding specificity *in vivo*. Further improvement of binding affinity and ADME properties are underway to develop new CYP46A1 ligands.

Acknowledgments

We thank Professor Thomas J. Brady (Nuclear Medicine and Molecular Imaging, Radiology, MGH and Harvard Medical School) and Dr. Lei Zhang (Pfizer, Inc.) for helpful discussion. This work was supported in part by United States Public Health Service Grants R01 GM062882 (to I.A.P),

Supplementary data

Supplementary data to this article can be found online at https://doi.org/10.1016/xxxx.

References

1. Reitz C, Alzheimer's disease and the amyloid cascade hypothesis: a critical review, *Int. J. Alzheimers Dis.* 2012; 2012: 369808.
2. Vance JE, Dysregulation of cholesterol balance in the brain: contribution to neurodegenerative diseases, *Dis. Model. Mech.* 2012; 5: 746-755.
3. Anchisi L, Dessi S, Pani A, Mandas A, Cholesterol homeostasis: a key to prevent or slow down neurodegeneration, *Front. Physiol.* 2013; 3.
4. Zhang J, Liu Q, Cholesterol metabolism and homeostasis in the brain, *Protein Cell* 2015; 6: 254-264.
5. Segatto M, Tonini C, Pfrieger FW, Trezza V, Pallottini V, Loss of mevalonate/cholesterol homeostasis in the brain: a focus on autism spectrum disorder and Rett syndrome, *Int. J. Mol. Sci.* 2019; 20: 3317.
6. Mast N, Saadane A, Valencia-Olvera A, Constans J, Maxfield E, Arakawa H, Li Y, Landreth G, Pikuleva IA, Cholesterol-metabolizing enzyme cytochrome P450 46A1 as a pharmacologic target for Alzheimer's disease, *Neuropharmacology* 2017; 123: 465-476.
7. Moutinho M, Nunes MJ, Rodrigues E, Cholesterol 24-hydroxylase: Brain cholesterol metabolism and beyond, *Biochim. Biophys. Acta* 2016; 1861: 1911-1920.
8. Papassotiropoulos A, Streffer JR, Tsolaki M, Schmid S, Thal D, Nicosia F, Iakovidou V, Maddalena A, Lütjohann D, Ghebremedhin E, Hegi T, Pasch T, Träxler M, Brühl A, Benussi L, Binetti G, Braak H, Nitsch RM, Hock C, Increased brain *β*-amyloid load, phosphorylated tau, and risk of alzheimer disease associated with an intronic CYP46 polymorphism, *Arch Neurol.* 2003; 60: 29-35.
9. Wang B, Zhang C, Zheng W, Lu Z, Zheng C, Yang Z, Wang L, Jin F, Association between a T/C polymorphism in intron 2 of cholesterol 24*S*-hydroxylase gene and Alzheimer's disease in Chinese, *Neurosci. Lett.* 2004; 369: 104-107.
10. Desai P, DeKosky ST, Kamboh MI, Genetic variation in the cholesterol 24-hydroxylase (CYP46) gene and the risk of Alzheimer's disease, *Neurosci. Lett.* 2002; 328: 9-12.
11. Kölsch H, Lütjohann D, Tulke A, Björkhem I, Rao ML, The neurotoxic effect of 24-hydroxycholesterol on SH-SY5Y human neuroblastoma cells, *Brain Res.* 1999; 818: 171-175.
12. Rantham Prabhakara JP, Feist G, Thomasson S, Thompson A, Schommer E, Ghribi O, Differential effects of 24-hydroxycholesterol and 27-hydroxycholesterol on tyrosine hydroxylase and α-synuclein in human neuroblastoma SH-SY5Y cells, *J.Neurochem.* 2008; 107: 1722-1729.
13. Zhao S, Liao W, Xu N, Xu H, Yu C, Liu X, Li C, Polar metabolite of cholesterol induces rat cognitive dysfunctions, *Neuroscience* 2009; 164: 398-403.
14. Mast N, White MA, Bjorkhem I, Johnson EF, Stout CD, Pikuleva IA, Crystal structures of substrate-bound and substrate-free cytochrome P450 46A1, the principal cholesterol hydroxylase in the brain, *Proc. Natl. Acad. Sci.* 2008; 105: 9546-9551.
15. Mast N, Charvet C, Pikuleva IA, Stout CD, Structural basis of drug binding to CYP46A1, an enzyme that controls cholesterol turnover in the brain, *J. Biol. Chem.* 2010; 285: 31783-31795.
16. Shafaati M, Mast N, Beck O, Nayef R, Heo GY, Björkhem-Bergman L, Lütjohann D, Björkhem I, Pikuleva IA, The antifungal drug voriconazole is an efficient inhibitor of brain cholesterol 24S-hydroxylase in vitro and in vivo, *J. Lipid Res.* 2010; 51: 318-323.
17. Mast N, Linger M, Clark M, Wiseman J, Stout CD, Pikuleva IA, In Silico and Intuitive Predictions of CYP46A1 Inhibition by Marketed Drugs with Subsequent Enzyme Crystallization in Complex with Fluvoxamine, *Molecular Pharmacology* 2012; 82: 824-834.
18. Ametamey SM, Honer M, Schubiger PA, Molecular imaging with PET, *Chem. Rev.* 2008; 108: 1501-1516.
19. Willmann JK, van Bruggen N, Dinkelborg LM, Gambhir SS, Molecular imaging in drug development, *Nat. Rev. Drug Discov.* 2008; 7: 591-607.

20. Miller PW, Long NJ, Vilar R, Gee AD, Synthesis of ^{11}C, ^{18}F, ^{15}O, and ^{13}N radiolabels for positron emission tomography, *Angew. Chem., Int. Ed.* 2008; 47: 8998-9033.
21. Rotstein BH, Liang SH, Holland JP, Collier TL, Hooker JM, Wilson AA, Vasdev N, $^{11}CO_2$ fixation: a renaissance in PET radiochemistry, *Chem. Commun.* 2013; 49: 5621-5629.
22. Rotstein BH, Liang SH, Placzek MS, Hooker JM, Gee AD, Dollé F, Wilson AA, Vasdev N, ^{11}C O bonds made easily for positron emission tomography radiopharmaceuticals, *Chem. Soc. Rev.* 2016; 45: 4708-4726.
23. Dahl K, Collier TL, Cheng R, Zhang X, Sadovski O, Liang SH, Vasdev N, "In-loop" [^{11}C]CO_2 fixation: Prototype and proof of concept, *J. Labelled Comp. Radiopharm.* 2018; 61: 252-262.
24. Deng X, Rong J, Wang L, Vasdev N, Zhang L, Josephson L, Liang SH, Chemistry for positron emission tomography: recent advances in ^{11}C-, ^{18}F-, ^{13}N-, and ^{15}O-labeling reactions, *Angew. Chem. Int. Ed.* 2019; 58: 2580-2605.
25. Downey J, Bongarzone S, Hader S, Gee AD, In-loop flow [11C]CO2 fixation and radiosynthesis of N,N′-[11C]dibenzylurea, *Journal of Labelled Compounds and Radiopharmaceuticals* 2018; 61: 263-271.
26. Chen Z, Mori W, Deng X, Cheng R, Ogasawara D, Zhang G, Schafroth MA, Dahl K, Fu H, Hatori A, Shao T, Zhang Y, Yamasaki T, Zhang X, Rong J, Yu Q, Hu K, Fujinaga M, Xie L, Kumata K, Gou Y, Chen J, Gu S, Bao L, Wang L, Collier TL, Vasdev N, Shao Y, Ma J-A, Cravatt BF, Fowler C, Josephson L, Zhang M-R, Liang SH, Design, synthesis, and evaluation of reversible and irreversible monoacylglycerol lipase positron emission tomography (PET) tracers using a "tail switching" strategy on a piperazinyl azetidine skeleton, *J. Med. Chem.* 2019; 62: 3336-3353.
27. Horkka K, Dahl K, Bergare J, Elmore CS, Halldin C, Schou M, Rapid and efficient synthesis of ^{11}C-labeled benzimidazolones using [^{11}C]carbon dioxide, *ChemistrySelect* 2019; 4: 1846-1849.
28. Koike T, Yoshikawa M, Kamiski H, Farnaby WJ, Takeda Pharmaceutical Co. Ltd., , 2013, pp. US20130090341.
29. Koike T, Kajita Y, Yoshikawa M, Ikeda S, Kimura E, Hasui T, Nishi T, Fukuda H, Takeda Pharmaceutical Co. Ltd., Japan, 2014, pp. WO2014092100.
30. Wager TT, Hou X, Verhoest PR, Villalobos A, Moving beyond rules: The development of a central nervous system multiparameter optimization (CNS MPO) approach to enable alignment of druglike properties, *ACS Chem. Neurosci.* 2010; 1: 435-449.
31. Mast N, Verwilst P, Wilkey CJ, Guengerich FP, Pikuleva IA, In vitro activation of cytochrome P450 46A1 (CYP46A1) by Efavirenz-related compounds, *J. Med. Chem.* 2019.
32. Waterhouse RN, Determination of lipophilicity and its use as a predictor of blood-brain barrier penetration of molecular imaging agents, *Mol. Imaging Biol.* 2003; 5: 376-389.
33. Patel S, Gibson R, In vivo site-directed radiotracers: a mini-review, *Nucl. Med. Biol.* 2008; 35: 805-815.
34. Pike VW, Considerations in the development of reversibly binding PET radioligands for brain imaging, *Curr. Med. Chem.* 2016; 23: 1818-1869.
35. Test No. 107: Partition Coefficient (n-octanol/water): Shake Flask Method, Organisation for Economic Cooperation and Development (OECD), Paris, 1995.